Quantum lattice Boltzmann simulation of expanding Bose-Einstein condensates in random potentials

S. Palpacelli[1] and S. Succi[2]
[1]*Dipartimento di Matematica, Università Roma Tre, Largo San Leonardo Murialdo 1, 00146 Roma, Italy*
[2]*Istituto Applicazioni del Calcolo, Viale Policlinico 137, 00161 Roma, Italy*
(Received 18 February 2008; published 20 June 2008)

The phenomenon of Anderson localization in expanding one-dimensional Bose-Einstein condensates is investigated by numerically solving the Gross-Pitaevskii equation with a random speckle potential. To this purpose, a quantum lattice Boltzmann (QLB) method is used, and compared with a standard Crank-Nicolson scheme. The QLB simulations show evidence of Anderson localization even for relatively low-energy condensates, with a healing length as large as one-tenth of the Thomas-Fermi length. Moreover, very long-time simulations, lasting up to 15 000 optical confinement periods, indicate that the Anderson localization degrades in time, although at a very slow pace. In particular, the inverse localization length is found to decay according to a $t^{-1/3}$ law. This lends support to the idea that localized wave functions, although not strictly ground states, represent extremely long-lived metastable states of the expanding condensate.

DOI: 10.1103/PhysRevE.77.066708 PACS number(s): 02.70.−c, 03.65.−w

I. INTRODUCTION

The study of the dynamics of Bose-Einstein condensates (BECs) in the presence of a random potential is a very active topic in modern condensed matter and atomic physics research. Recently, a large number of experimental and numerical studies have been devoted to the localization properties of Bose gases [1–9]. It is well known that disorder can profoundly affect the behavior of quantum systems, Anderson localization being one of the most fascinating phenomena in point [10]. Back in 1958, Anderson showed that the eigenstates of single quantum particles in a weak random potential can become localized, which means that the corresponding wave functions exhibit an exponential decay at large distances [1]. Indeed, strong suppression of transport phenomena in expanding BECs in the presence of disorder has been recently observed experimentally and confirmed by numerical simulations [3–8]. However, this suppression of transport is not due to Anderson localization, but rather to the fragmentation of the BEC, as it gets trapped between the peaks of the random potential. In Ref. [11], a theoretical and numerical study prescribes the conditions under which a one-dimensional BEC can exhibit Anderson localization. These conditions basically amount to requiring that the amplitude of the random potential be sufficiently large to promote destructive interference between freely propagating plane waves, and yet significantly smaller than the condensate energy, so as to avoid disruptive fragmentation of the wave function. In addition, the correlation length of the random potential should be smaller than the healing length of the condensate (the scale below which kinetic energy is dominant), so that noise can couple to a sizable fraction of the spectrum of kinetic-energy carriers.

The aim of this work is to further investigate these conditions by means of a quantum lattice Boltzmann (QLB) model. Originally, the QLB method was developed starting from a formal analogy between the Dirac equation and a Boltzmann equation for a complex distribution function [12–14]. A major feature of the QLB model is that unitarity and stability can be achieved with a time step scaling linearly with mesh size rather than quadratically as in most explicit schemes for quantum wave functions [15]. Recently, a multidimensional formulation of the QLB scheme has been proposed and also extended to the case of nonlinear interactions, as described by the Gross-Pitaevskii equation (GPE) [16,17].

In the past decade, many different numerical approaches have been applied to the solution of the time-dependent GPE, e.g., a particle-inspired scheme proposed by Chiofalo *et al.* [18,19], finite difference methods proposed by Ruprecht *et al.* [20], Ensher *et al.* [21], and Wang [22], and a time-splitting spectral (TSSP) method developed by Bao and co-workers initially for the Schrödinger equation in the semiclassical regime [23,24] and then extended to the GPE [25,26]. In particular, the TSSP method shows good properties of accuracy and efficiency.

In the present work we explore the use of the QLB method for the case of nonlinear interactions with random potentials. A systematic comparison with the classical Crank-Nicolson (CN) scheme is also presented, in order to validate QLB numerical results and assess the computational performances at different space-time resolutions. Finally, we investigate the mechanism by which the localized state of the BEC is modified by the residual self-interaction in the (very) long-time evolution of the condensate.

II. REVIEW OF THE QUANTUM LATTICE BOLTZMANN MODEL

The quantum lattice Boltzmann model proposed in Refs. [12–14] is based on a formal analogy between the Dirac equation and the discrete kinetic equation known as the lattice Boltzmann equation. In particular, it is possible to show that the nonrelativistic Schrödinger equation ensues from the relativistic Dirac equation in the adiabatic limit where antisymmetric fast modes are enslaved to the symmetric slow ones.

The procedure outlined in Ref. [12] to extend the model to two and three spatial dimensions has been recently tested

against numerical simulations [16]. An imaginary-time version of the QLB model has also been proposed [17] to compute the ground state solution of the Gross-Pitaevskii equation by applying, to the time-dependent GPE, a transformation known as Wick rotation [27–29].

The real-time QLB model

Let us recall the main ideas behind the quantum lattice Boltzmann scheme in one dimension. Consider the Dirac equation in one dimension. Using the Majorana representation [30] and projecting upon chiral eigenstates, the Dirac equation reads

$$\partial_t u_{1,2} + c\partial_z u_{1,2} = \omega_c d_{2,1} + i g u_{1,2},$$

$$\partial_t d_{1,2} - c\partial_z d_{1,2} = -\omega_c u_{2,1} + i g d_{1,2}, \tag{1}$$

where $u_{1,2}$ and $d_{1,2}$ are complex wave functions composing the Dirac quadrispinor $\psi=(u_1,u_2,d_1,d_2)^T$, and $\omega_c=mc^2/\hbar$ is the Compton frequency, $g=qV/\hbar$ is the space-dependent frequency coupling to the external potential V, and q is the particle electric charge. Since we restrict our attention to electrostatic potentials, the spinorial indices will be dropped in the following.

As observed in Ref. [12], Eq. (1) is a discrete Boltzmann equation for a pair of complex wave functions u and d. In particular, the propagation step consists of streaming u and d along the z axis with opposite speeds $\pm c$, while the collision step is performed according to the scattering matrix defined by the right-hand side of Eq. (1).

Nonrelativistic motion is reproduced by the model in the adiabatic (low-frequency) limit:

$$|\omega - \omega_c| \ll |\omega_c + g|, \tag{2}$$

where ω is the typical frequency (energy) of the solution ψ. With the additional constraint of "small" potential interaction

$$|g| \ll \omega_c, \tag{3}$$

it can be shown that the "slow" mode (to be defined shortly) dynamics is governed by the Schrödinger equation for a spinless particle of mass m. In particular, under the unitary transformation

$$\phi^{\pm} = \frac{1}{\sqrt{2}}\exp(i\omega_c t)(u \pm id),$$

from Eq. (1) it is easy to check that the following equations are satisfied:

$$\partial_t \phi^+ + c\partial_z \phi^- = ig\phi^+,$$

$$\partial_t \phi^- + c\partial_z \phi^+ = 2i\omega_c \phi^- + ig\phi^-. \tag{4}$$

From Eq. (4), after adiabatic elimination of the "fast" antisymmetric mode

$$|\partial_t \phi^-| \ll |2\omega_c + g||\phi^-|,$$

we obtain

$$i\hbar\partial_t\phi^+ = -\frac{\hbar c^2}{2\omega_c}\partial_z\left(\frac{2\omega_c}{2\omega_c+g}\partial_z\phi^+\right) - qV\phi^+$$

$$\approx -\frac{\hbar^2}{2m}\partial_z^2\phi^+ - qV\phi^+, \tag{5}$$

where the last approximation in Eq. (5) is valid in the small potential interaction limit given by Eq. (3).

The QLB scheme is obtained by integrating Eq. (1) along the characteristics of u and d, respectively, and approximating the right-hand side integral by using the trapezoidal rule. Assuming $\Delta z=c\Delta t$, the following scheme is obtained:

$$\hat{u} - u = \frac{\tilde{m}}{2}(d + \hat{d}) + \frac{i\tilde{g}}{2}(u + \hat{u}),$$

$$\hat{d} - d = -\frac{\tilde{m}}{2}(u + \hat{u}) + \frac{i\tilde{g}}{2}(d + \hat{d}), \tag{6}$$

where $\hat{u}=u(z+\Delta z,t+\Delta t)$, $\hat{d}=d(z-\Delta z,t+\Delta t)$, $u=u(z,t)$, $d=d(z,t)$, $\tilde{m}=\omega_c\Delta t$, and $\tilde{g}=g\Delta t$. The linear system of Eq. (6) is algebraically solved for $\hat{u}$ and $\hat{d}$ and yields the explicit scheme

$$\hat{u} = au + bd,$$

$$\hat{d} = ad - bu, \tag{7}$$

where

$$a = (1 - \Omega/4)/(1 + \Omega/4 - i\tilde{g}), \quad b = \tilde{m}/(1 + \Omega/4 - i\tilde{g}),$$

with $\Omega=\tilde{m}^2-\tilde{g}^2$. Here $\tilde{m}=\omega_c\Delta t$ represents the dimensionless Compton frequency. Note that, since $|a|^2+|b|^2=1$, the collision matrix is unitary, the method is unconditionally stable and norm preserving. In particular, the quantity $\|\phi^+\|^2+\|\phi^-\|^2$, where $\|\cdot\|$ indicates the L^2 norm, is kept at unit value throughout the evolution. It follows that $\|\phi^+\|^2$ cannot be preserved during the evolution. Indeed, we have $\|\phi^-\| \ll \|\phi^+\|$ with both terms oscillating in such a way that $\|\phi^+\|^2+\|\phi^-\|^2=1$.

III. THE GROSS-PITAEVSKII EQUATION

At zero temperature, the dynamics of a trapped Bose-Einstein condensate is described by the time-dependent Gross-Pitaevskii equation. The GPE for a quantum wave function $\psi(\boldsymbol{r},t)$, with $\boldsymbol{r}=(x,y,z)^T \in \mathbb{R}^3$, reads as follows:

$$i\hbar\partial_t\psi(\boldsymbol{r},t) = \left(-\frac{\hbar^2}{2m}\Delta_r + V_{\text{ext}}(\boldsymbol{r}) + NU_0|\psi(\boldsymbol{r},t)|^2\right)\psi(\boldsymbol{r},t), \tag{8}$$

where m is the atomic mass, $U_0=4\pi\hbar^2 a/m$ is the coupling strength, a is the scattering length, N is the number of particles in the condensate, and $V_{\text{ext}}(\boldsymbol{r})$ is the external trapping potential.

Typically, the external potential is taken in the form of a harmonic trap:

$$V_{\text{ext}}(x,y,z) = \frac{1}{2}m(\omega_x^2 x^2 + \omega_y^2 y^2 + \omega_z^2 z^2).$$

The three-dimensional GPE can be easily reduced to one dimension for a particular choice of the harmonic trap [18,31–34]. In particular, for $\omega_x = \omega_y \equiv \omega_\perp$ and $\omega_z \ll \omega_\perp$, the GPE of Eq. (8) is transformed into

$$i\hbar\partial_t\psi(z,t) = \left(-\frac{\hbar^2}{2m} + V_{\text{ext}}(z) + NU_1|\psi(z,t)|^2\right)\psi(z,t), \quad (9)$$

where $U_1 = 2a\hbar\omega_\perp$ is the one-dimensional coupling constant equivalent to the three-dimensional one and $V_{\text{ext}}(z) = (1/2)m\omega_z^2 z^2$. In order to numerically solve Eq. (9) by using the QLB and CN schemes, the so-called QLB scaling [17] is applied to Eq. (9).

QLB scaling

The QLB scaling is defined by

$$\hat{t} = \frac{t}{\delta_t}, \quad \hat{z} = \frac{z}{\delta_z}, \quad \hat{\psi}(z,t) = (\delta_z)^{1/2}\psi(z,t), \quad \hat{\omega}_z = \omega_z\delta_t,$$

where δ_z and δ_z are the discretization steps in physical units. From $\hat{\omega}_z = \omega_z\delta_t$, the time step is readily computed, $\delta_t = \tilde{\omega}_z/\omega_z$. As observed in Ref. [17], since the relation $\delta_z = c\,\delta_t$ must hold, it is apparent that in order to simulate physical situations c must be taken much smaller than the physical light speed. Otherwise, we would need a very small time step to achieve a reasonable δ_z. In particular, from the definition of the model parameter $\tilde{m} = \omega_c\delta_t = (mc^2/\hbar)\delta_t$, we have

$$c^2 = \frac{\tilde{m}\hbar}{m\delta_t},$$

and then

$$\delta_z = c\,\delta_t = \left(\frac{\tilde{m}\hbar}{m\delta_t}\right)^{1/2}\delta_t.$$

By applying this scaling to Eq. (9) and removing all the ~, we obtain

$$i\partial_t\psi(z,t) = \left(-\frac{1}{2\tilde{m}}\partial_z^2 + \frac{1}{2}\tilde{m}\omega_z^2 z^2 + \beta_{\text{QLB}}|\psi(z,t)|^2\right)\psi(z,t),$$

where the nonlinearity coupling constant β_{QLB} is given by

$$\beta_{\text{QLB}} = \frac{2a_z^2 a\omega_z N}{\delta_z a_\perp^2},$$

with $a_z = \sqrt{\hbar/(m\omega_z)}$ and $a_\perp = \sqrt{\hbar/(m\omega_\perp)}$. From the above expression, it is clear that the adiabatic assumption underlying the QLB theory sets a limit on the strength of the nonlinear interactions, i.e., on the number of bosons, N. More precisely, the high-energy components of the wave functions evolve according to a second-order hyperbolic (Klein-Gordon) equation, rather than to the first-order parabolic (Schrödinger) diffusive dynamics.

IV. ANDERSON LOCALIZATION OF EXPANDING BEC IN SPECKLE POTENTIAL

The aim of this work is to apply the QLB scheme to the study of an expanding BEC in the presence of disorder. As is well known, quantum systems can be highly affected by disorder, one of the most famous phenomena that may occur being Anderson localization [10], whereby the eigenstates of single quantum particles in a weak random potential can become localized, i.e., the eigenstates exhibit an exponential decay at large distances [1]. In one spatial dimension, the entire wave function is localized, i.e. all eigenstates are localized. Recently, both experimental and numerical studies have been devoted to the localization of Bose gases [1–7] in order to fully understand the interplay between nonlinear interactions and disorder. The strength of the interaction is characterized by the inverse ratio of the initial healing length $\xi_h = \hbar/\sqrt{4m\mu}$ to the Thomas-Fermi length $L_{\text{TF}} = \sqrt{2\mu/m\omega_z^2}$, where μ is the chemical potential, m the boson mass, and ω_z the longitudinal frequency of the optical trap [1]. The properties of a random potential are summarized by its intensity V_R and correlation length σ_R.

As shown in Ref. [11], for $\sigma_R < \xi_h$ and for a weak disorder $V_R/\mu < 1$, a one-dimensional BEC can exhibit Anderson localization. As observed in Ref. [11], localization of a BEC in a random potential was already reported in Refs. [3–5]. However, in this case, suppression of transport was not due to Anderson localization, but rather to the fragmentation of the BEC, as a result of trapping between the peaks of the potential.

Following the model proposed in Ref. [11], we consider a one-dimensional Bose-Einstein condensate trapped in a harmonic potential in the presence of a random potential $V(z)$. The corresponding Gross-Pitaevskii equation reads as follows:

$$i\hbar\partial_t\psi(z,t) = \left(-\frac{\hbar^2}{2m}\partial_z^2 + \frac{1}{2}m\omega_z^2 z^2 + V(z) + NU_1|\psi(z,t)|^2 - \mu\right)\psi(z,t), \quad (10)$$

where U_1 is the coupling constant and μ is the chemical potential. The random potential $V(z)$ is taken in the form of a one-dimensional speckle potential [6,35–37], with a truncated negative exponential single-point distribution:

$$P(V) = \frac{\exp(-[V+V_R]/V_R)}{V_R}\Theta\left(\frac{V}{V_R}+1\right), \quad (11)$$

where Θ is the Heaviside step function. The average of V over the disorder vanishes, while $\langle V^2\rangle = V_R$. The correlation function $C(z) = \langle V(z')V(z'+z)\rangle$ can be written as a function of the correlation length of the potential, σ_R. For a speckle potential produced by diffraction through a square aperture [5,35], the autocorrelation function reads as follows:

$$C(z) = \langle V(z')V(z'+z)\rangle = V_R^2\text{sinc}^2(z/\sigma_R), \quad (12)$$

where $\text{sinc}(x) := \sin(x)/x$ and $\langle\cdot\rangle$ stands for integration over z' and averaging over many realizations.

Initially, the BEC is assumed to be at equilibrium in the harmonic trap; then the harmonic trap is removed and the BEC starts to freely expand. At time $t \gg 1/\omega_z$, the random potential is switched on. Starting from this model, in Ref. [11] it is shown that, for $\sigma_R < \xi_h$ and when the random potential satisfies the condition

$$V_R \ll \mu(\xi_h/\sigma_R)^{1/2}, \tag{13}$$

the BEC wave function undergoes Anderson localization. In particular, the large-distance asymptotic behavior of the wave-function density $n(z)$ is given by

$$n(z) \propto |z|^{-3/2}\exp[-2\gamma(1/\xi_h)|z|], \tag{14}$$

where $\gamma(k)=1/L(k)$ is the Lyapunov exponent and $L(k)$ is the localization length. In Ref. [11], an approximation to $\gamma(k)$ is computed and related to the correlation properties of the disorder. For the speckle potential used in this work, one has [11]

$$\gamma(k) \sim \gamma_0(k)(1-|k|\sigma_R)\Theta(1-|k|\sigma_R), \quad \gamma_0(k) = \frac{\pi m^2 V_R^2 \sigma_R}{2\hbar^4 k^2}. \tag{15}$$

V. NUMERICAL RESULTS

The time evolution of the BEC wave function is traced by solving Eq. (10) by means of the QLB and CN schemes. We observe that the QLB model is designed so as to solve Eq. (10) in the QLB scaling, whereby $c\Delta t/\Delta z=1$, so that Δz and Δt scale linearly with each other. The unitarity of the collision matrix implies that the scheme is unconditionally stable and norm preserving for any value of $\Delta z=c\Delta t$. The CN is an implicit scheme, and hence unconditionally stable, although its accuracy depends on the diffusion Courant-Friedrichs-Lewy (CFL) coefficient $C_D=\frac{D\Delta t}{(\Delta z)^2}$, where $D=\hbar/(2m)$ and the potential CFL coefficient $C_V=\frac{V\Delta t}{\hbar}$, where $V=V_R+NU_1\max_z(|\psi(z)|^2)$. We solve Eq. (10) with the QLB scaling by using both QLB and CN schemes and we increase time and space resolution while keeping $\Delta z=\Delta t$ ($c=1$ in atomic units) as required by the QLB model.

As observed in Sec. II, the real-time QLB scheme solves the GPE in the limit of small potential interaction. Hence, large values for the coupling constant β_{QLB} violate the adiabatic assumption. This implies limitations to the ratio between L_{TF} and ξ_h, where $L_{\mathrm{TF}}=\sqrt{2\mu/m\omega_z^2}$ is the Thomas-Fermi half-length. In practice, the QLB method is constrained to $\lambda \equiv L_{\mathrm{TF}}/\xi_h \sim 10$.

In particular, for the present simulations, the parameters are set as follows:

$$\omega_z = 5\times 10^{-3}, \quad \beta_{\mathrm{QLB}} = 2, \quad \tilde{m} = 1/4.$$

This setup delivers $\mu=0.019\,43$, $L_{\mathrm{TF}}=78.85$, and $\xi_h=7.17$. The domain length is set to $L=32\,000\sim 400L_{\mathrm{TF}}$ and the simulation span at $T=150/\omega_z=30\,000$. As a result, $\lambda=10.997$ and we set $V_R=0.2\mu$ and $\sigma_R=0.5\xi_h$, so that $\sigma_R<\xi_h$ and the conditions of Eq. (13) are satisfied.

As previously mentioned, localization of an expanding BEC in random potentials has been experimentally observed in Refs. [3–5,8,9]. However, in those experiments, the parameter setting does not satisfy the condition $\sigma_R<\xi_h$ and the constraint of Eq. (13), which are crucial in order to detect the Anderson localization phenomenon [11]. Nonetheless, the parameter setting proposed in Ref. [11] and used here is definitely accessible in current experiments. Indeed, recent experiments reported in Ref. [38] have investigated this range of parameters and reported clear evidence of Anderson localization, in good agreement with the theoretical predictions of Refs. [11,39]. In particular, in the experiment of Ref. [38], the authors consider a BEC composed of $N=1.7\times 10^4$ atoms of ^{87}Rb with an initial chemical potential $\mu/(2\pi\hbar)=219$ Hz. The BEC is initially trapped by an elongated harmonic potential with a transverse frequency $\omega_\perp/(2\pi)=70$ Hz and a longitudinal frequency $\omega_z/(2\pi)=5.4$ Hz. This implies a Thomas-Fermi half-length $L_{\mathrm{TF}}=41.75$ μm and an initial healing length $\xi_h=0.364$ μm, thus yielding a separation scale $\lambda=114$. The speckle potential can be accurately controlled in order to attain specific values for the mean intensity V_R and correlation length σ_R. In Ref. [38], the mean intensity is tuned so that V_R/μ varies in the range $0.07-0.34$, while the correlation length is set at $\sigma_R=0.26$ μm, thus satisfying the condition $\sigma_R<\xi_h$ and the constraint of Eq. (13). With this setting, the exponential localization is clearly observed and the localization length L_{loc} is found to vary from about 2 to 0.25 mm, while the mean intensity of the speckle potential V_R is increased.

In our simulations, we are considering a more weakly interacting BEC, which could be experimentally achieved by decreasing the interatomic interaction either by density control (i.e., lower number of atoms) or by Feshbach resonances [38]. In particular, by leaving all the other parameters unchanged, we are simulating a BEC with $\mu/(2\pi\hbar)=21$ Hz, which delivers $L_{\mathrm{TF}}=13$ μm and $\xi_h=1.18$ μm, thus yielding $\lambda\sim 11$. As we shall see below, with this setting we obtain a localization length $L_{\mathrm{loc}}=1.19$ mm for $V_R/\mu=0.2$. In conclusion, our set of parameters is representative of current BEC experiments, although with possibly a weaker nonlinearity, i.e., narrower separation between the outer and inner length scales, L_{TF} and ξ_h, respectively. As we shall demonstrate, a scale separation $\lambda\sim 10$ is nonetheless sufficient to yield clear evidence of Anderson localization.

In Fig. 1, we present the averaged wave function for five different values of the separation parameter λ. From this figure, a clear delocalization trend with decreasing values of λ is observed.

The separation parameter λ is changed by tuning the coupling constant β_{QLB}. By changing β_{QLB}, the chemical potential μ is also changed and, consequently, L_{TF} and ξ_h are modified. Parameters are chosen in such a way that the ratios V_R/μ and σ_R/ξ_h are kept at 0.2 and 0.5, respectively. Discretization steps are chosen so that a sufficient resolution is achieved. In particular, numerical experiments show that satisfactory results are obtained for $R>5$, where $R\equiv\xi_h/\Delta z$ is the resolution parameter. This has been set to the following values:

$$\lambda = 1, \quad R = 23.78 \quad (\Delta z = 1);$$

$$\lambda = 5, \quad R = 10.63 \quad (\Delta z = 1);$$

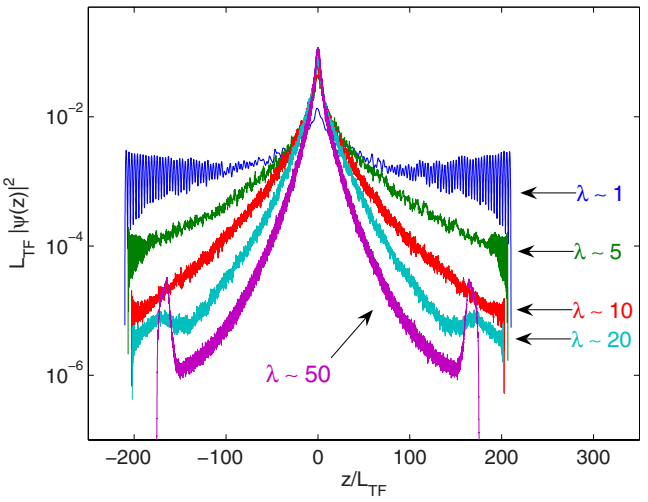

FIG. 1. (Color online) Averaged wave-function densities computed by the QLB method for five different values of the ratio $\lambda \equiv L_{\mathrm{TF}}/\xi_h = 1, 5, 10, 20, 50$ (top down). Parameters are set as follows: $\omega_z = 5 \times 10^{-3}$, $\tilde{m} = 1/4$, $V_R = 0.2\mu$, $\sigma_R = 0.5\xi_h$, and $T = 150/\omega_z$. The delocalization trend at increasing values of λ is well visible.

$$\lambda = 10, \quad R = 7.16 \quad (\Delta z = 1);$$

$$\lambda = 20, \quad R = 10.62 \quad (\Delta z = 0.5);$$

$$\lambda = 50, \quad R = 6.72 \quad (\Delta z = 0.5).$$

For $\lambda > 10$, an unphysical pileup on the tails of the wave function is observed, which is due to the lack of adiabaticity of the fast (high-frequency) modes. As we shall see, this problem also arises for $\lambda \sim 10$, when the grid resolution is not sufficient, i.e., whenever the wavelength of the highest frequencies becomes comparable with the lattice spacing.

It is instructive to investigate the effects of spatial resolution, as measured by the parameter R, representing the number of nodal points covering the initial healing length. We start with an under-resolved situation, $R = 0.448$ (corresponding to $N_g = 2000$ nodal points), and subsequently increase the resolution up to $R = 28.68$ ($N_g = 128\,000$). While increasing the spatial resolution, we also increase the time resolution by keeping $\Delta t = \Delta z$. The elapsed time spent by the QLB and CN methods is quite similar at all resolutions, with a mild tendency of QLB to outperform CN at high resolutions (5058 versus 6242 CPU seconds for $N_g = 128\,000$ on a standard PC Intel Pentium 4, 3 GHz).

The wave-function density is computed by averaging over the solutions obtained with 100 realizations of the speckle potential. In Figs. 2 and 3, the averaged wave-function densities computed by the QLB and CN methods, respectively, at the four spatial resolutions ($N_g = 2000, 8000, 32\,000, 128\,000$) are shown and compared with the asymptotic behavior given by Eq. (14). In QLB simulations, pileup at high frequencies and large distances is observed (see Fig. 2), which is due to the failure of the adiabaticity assumption at high energies. The CN solution, on the other hand, shows a very different behavior at low resolution,

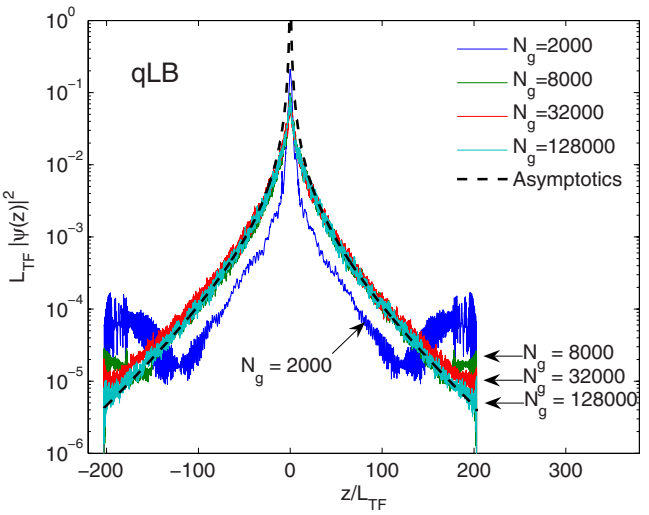

FIG. 2. (Color online) Averaged wave-function density computed by the QLB method at four different resolutions. The numerical results are compared with the long-tail asymptotic behavior given by Eq. (14). Parameters are set as follows: $\omega_z = 5 \times 10^{-3}$, $\beta_{\mathrm{QLB}} = 2$, $\tilde{m} = 1/4$, $V_R = 0.2\mu$, $\sigma_R = 0.5\xi_h$, $\lambda = 10.997$, and $T = 150/\omega_z$.

namely, an overlocalization of the wave function (see Fig. 3 for $N_g = 2000$). This signals the potential "danger" that under-resolved CN simulations may *overestimate* Anderson localization.

In Fig. 4, the averaged wave-function densities, computed at the four different resolutions by the QLB and CN methods, respectively, are compared. We observe that for $N_g \gtrsim 32\,000$ the two methods are in good agreement with each other, as well as with the predicted asymptotic behavior.

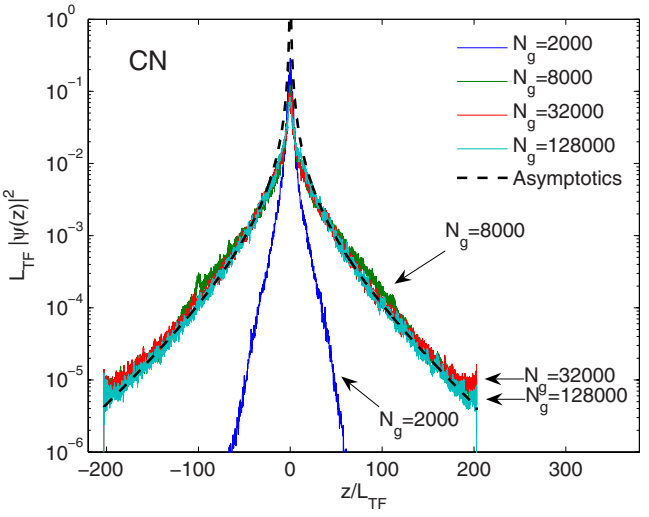

FIG. 3. (Color online) Averaged wave-function density computed by the CN method using the QLB scaling at four different resolutions. The numerical results are compared with the long-tail asymptotic behavior described by Eq. (14). Parameters are set as follows: $\omega_z = 5 \times 10^{-3}$, $\beta_{\mathrm{QLB}} = 2$, $\tilde{m} = 1/4$, $V_R = 0.2\mu$, $\sigma_R = 0.5\xi_h$, $\lambda = 10.997$, and $T = 150/\omega_z$.

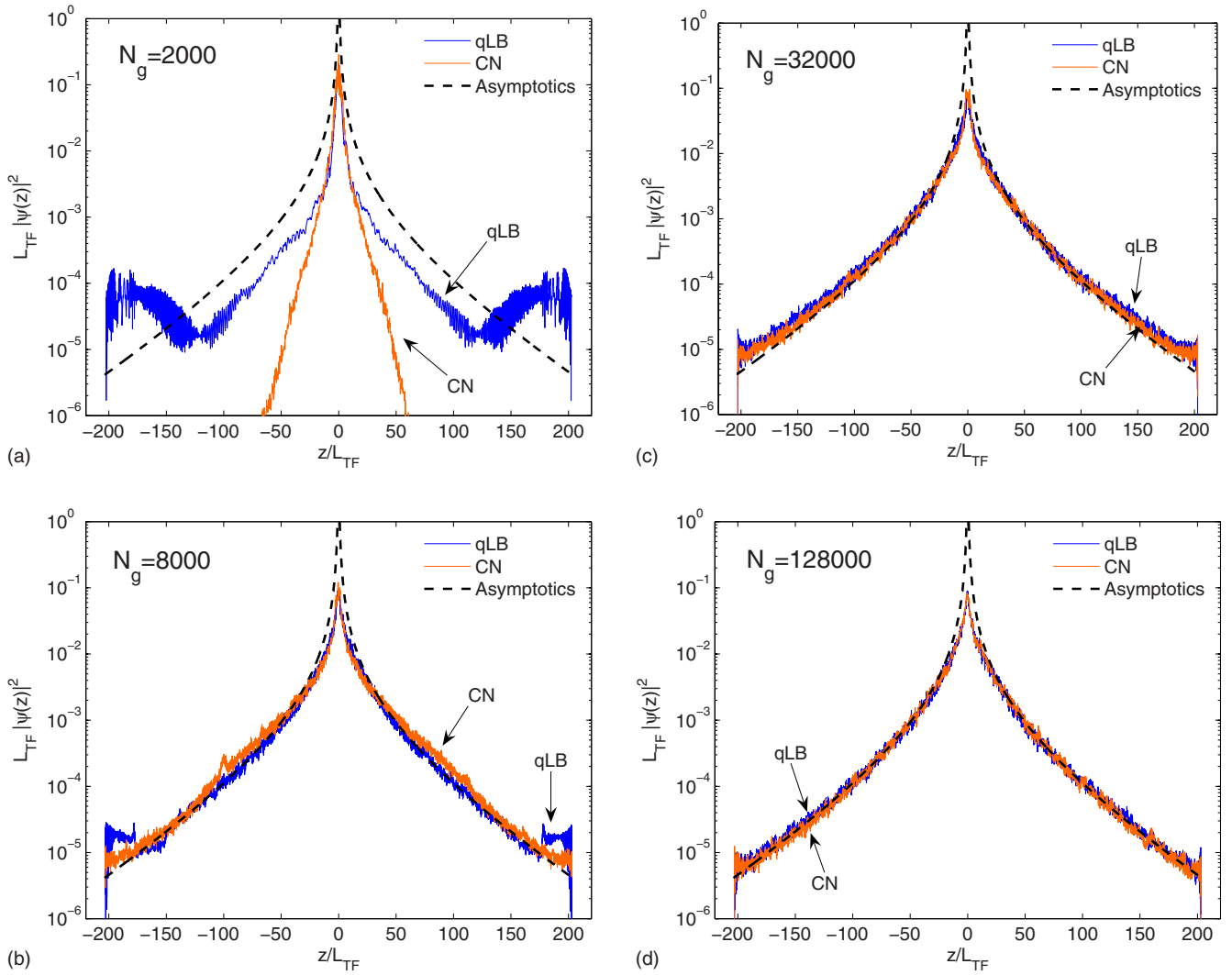

FIG. 4. (Color online) Comparison between the averaged wave-function densities computed by the QLB and CN methods at four different resolutions. The numerical results are compared with the long-tail asymptotic behavior described by Eq. (14). Parameters are set as follows: $\omega_z=5\times10^{-3}$, $\beta_{\mathrm{QLB}}=2$, $\tilde{m}=1/4$, $V_R=0.2\mu$, $\sigma_R=0.5\xi_h$, $\lambda=10.997$, $T=150/\omega_z$. $N_g=$ (a) 2000, (b) 8000, (c) 32 000, and (d) 128 000.

VI. LONG-TIME DEPLETION

In Ref. [11], it is argued that the expanding and then localized BEC might be a long-lived metastable state rather than a true ground-state solution. If so, the residual self-interaction should cause a long-term depletion of the BEC. The question arises as to whether such long-term depletion really occurs, and, if so, on which time scale. In order to explore this question, we have performed very long-time simulations up to time $t=15\,000/\omega_z$, 100 times longer than in the previous literature. As previously mentioned, the QLB scheme is norm preserving due to the unitarity of the collision matrix, a property that has been verified also for such long simulations. The global norm $\|\phi^+\|^2+\|\phi^-\|^2$ is observed to remain at a unit value up to the sixth digit at the end of our longest simulation (3×10^6 time steps); in particular the mean value is $\langle\|\phi^+\|^2+\|\phi^-\|^2\rangle=1.000\,000\,19$ with a standard deviation of 1.47×10^{-7}, to be compared with the value 3.72×10^{-8} after 3×10^5 time steps. These values indicate that the QLB solver does not seem to suffer from any significant degradation in the course of the very long-time simulations.

The averaged wave-function densities at times $t=1500/\omega_z$ and $15\,000/\omega_z$ are compared with the one obtained at time $t=150/\omega_z$, as shown in Fig. 5. The BEC is still well localized, but clearly on the way to losing its localization. In particular, by fitting the numerical wave-function densities with the analytical curve $n(z)\propto|z|^{-3/2}\exp(-2\gamma|z|)$, the following time-decay law for γ is found (see Fig. 6):

$$L_{\mathrm{TF}}\gamma(t)=\frac{0.055}{(\omega_z t)^{1/3}}. \tag{16}$$

In Fig. 5, the analytical curves obtained with the values of γ given by Eq. (16) for $t\omega_z=150$, 1500, and 15 000 are also shown. In Fig. 6, numerical results for $L_{\mathrm{TF}}\gamma$ as a function of $\omega_z t$ are reported and compared with the scaling law Eq. (16). For this numerical test, we used the QLB scheme with $N=32\,000$ nodal points, while other parameters are set as before. Although a direct comparison with experimental results

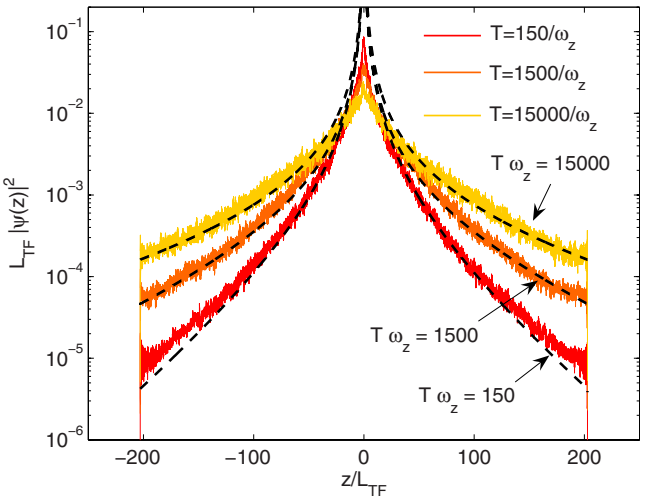

FIG. 5. (Color online) Averaged wave-function densities computed by the QLB method with $N=32\,000$ discretization points up to times $T=150/\omega_z$, $1500/\omega_z$, and $15\,000/\omega_z$. Parameters are set as follows: $\omega_z=5\times10^{-3}$, $\beta_{\mathrm{QLB}}=2$, $\tilde{m}=1/4$, $V_R=0.2\mu$, $\sigma_R=0.5\xi_h$, and $\lambda=10.997$.

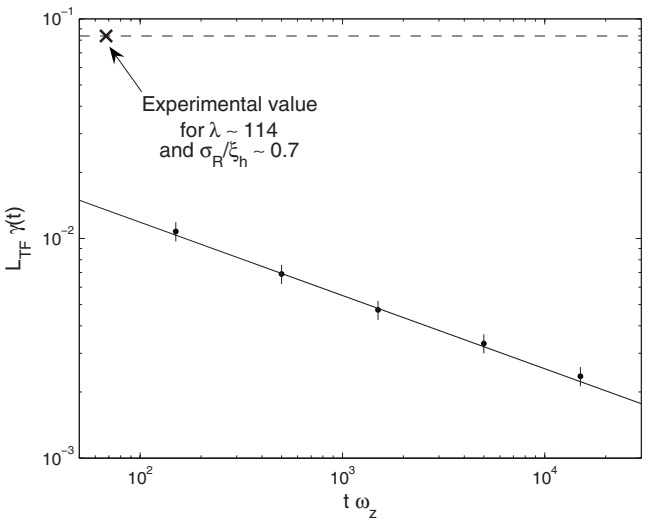

FIG. 6. Numerical values of $L_{\mathrm{TF}}\gamma$ at different times compared with the decay law of Eq. (16). Parameters are set as follows: $\omega_z=5\times10^{-3}$, $\beta_{\mathrm{QLB}}=2$, $\tilde{m}=1/4$, $V_R=0.2\mu$, $\sigma_R=0.5\xi_h$, and $\lambda=10.997$. Error bars indicate the min-max values over the ensemble of realizations. The point $\times$ indicates the experimental result obtained in Ref. [38] for $V_R/\mu=0.2$, as in our simulation, but for a different setting of λ and σ_R/ξ_h, which take the values 114 and 0.7, respectively.

reported in Ref. [38] is not possible, since we are simulating a BEC with a weaker nonlinearity ($\lambda\sim11$ instead of $\lambda\sim114$) and with a different value for the ratio σ_R/ξ_h, in Fig. 6 we report the experimental value obtained in Ref. [38] for $\lambda=114$, $\sigma_R/\xi_h\sim0.7$, and $V_R/\mu=0.2$. This last parameter is the same as in our simulations. The experimental result corresponds to a localization length of about $L_{\mathrm{loc}}=0.5$ mm, while in our simulation, we obtain $L_{\mathrm{loc}}=1.19$ mm. The pictures show a clear delocalization trend in the very long-term evolution of the condensate, thereby supporting the conjecture that Anderson localization is a long-lived *metastable* state of the expanding condensate.

VII. CONCLUSIONS

Summarizing, we have investigated Anderson localization effects in one-dimensional Bose-Einstein condensates subject to random potentials. To this purpose a QLB scheme has been used, and compared with the standard Crank-Nicolson method. The adiabatic approximation underlying the QLB theoretical framework sets limits on the strength of the self-interaction potential, which result in a smaller separation between the Thomas-Fermi scale and the healing length, as compared to typical experimental values. The QLB simulations indicate that scale separations $L_{\mathrm{TF}}/\xi_h\sim10$ are sufficient to show clear evidence of Anderson localization. In addition, very long-time simulations, 100 times longer than in the previous literature, show evidence of a progressive, if very slow ($t^{-1/3}$), delocalization of the condensate. The QLB scheme is found to perform competitively with respect to the CN scheme even in one dimension, and it is consequently expected to significantly outperform it in higher dimensions [17].

ACKNOWLEDGMENTS

Useful discussions with R. Spigler are kindly acknowledged. The authors are grateful to L. Sanchez-Palencia for many valuable hints and clarifications and also for making Ref. [38] available to us prior to publication.

[1] L. Sanchez-Palencia, Phys. Rev. A **74**, 053625 (2006).
[2] P. Lugan, D. Clément, P. Bouyer, A. Aspect, M. Lewenstein, and L. Sanchez-Palencia, Phys. Rev. Lett. **98**, 170403 (2007).
[3] D. Clément, A. F. Varón, M. Hugbart, J. A. Retter, P. Bouyer, L. Sanchez-Palencia, D. M. Gangardt, G. V. Shlyapnikov, and A. Aspect, Phys. Rev. Lett. **95**, 170409 (2005).
[4] C. Fort, L. Fallani, V. Guarrera, J. E. Lye, M. Modugno, D. S. Wiersma, and M. Inguscio, Phys. Rev. Lett. **95**, 170410 (2005).
[5] D. Clément, A. F. Varón, J. A. Retter, L. Sanchez-Palencia, A. Aspect, and P. Bouyer, New J. Phys. **8**, 165 (2006).
[6] M. Modugno, Phys. Rev. A **73**, 013606 (2006).
[7] E. Akkermans, S. Ghosh, and Z. Musslimani, J. Phys. B **41**, 045302 (2008).
[8] T. Schulte, S. Drenkelforth, J. Kruse, W. Ertmer, J. Arlt, K. Sacha, J. Zakrzewski, and M. Lewenstein, Phys. Rev. Lett. **95**, 170411 (2005).
[9] J. E. Lye, L. Fallani, M. Modugno, D. S. Wiersma, C. Fort, and M. Inguscio, Phys. Rev. Lett. **95**, 070401 (2005).
[10] P. W. Anderson, Phys. Rev. **109**, 1492 (1958).
[11] L. Sanchez-Palencia, D. Clément, P. Lugan, P. Bouyer, G. V. Shlyapnikov, and A. Aspect, Phys. Rev. Lett. **98**, 210401

(2007).
[12] S. Succi and R. Benzi, Physica D **69**, 327 (1993).
[13] S. Succi, in *Cellular Automata*, Lecture Notes in Computer Science Vol. 2493, edited by Stefania Bandini, Bastien Chopard, and Marco Tomassini (Springer-Verlag, Berlin, 2002), p. 114.
[14] S. Succi, Phys. Rev. E **53**, 1969 (1996).
[15] *Time Dependent Methods for Quantum Dynamics*, edited by K. C. Kulander (North-Holland, Amsterdam, 1991).
[16] S. Palpacelli and S. Succi, Phys. Rev. E **75**, 066704 (2007).
[17] S. Palpacelli, S. Succi, and R. Spigler, Phys. Rev. E **76**, 036712 (2007).
[18] M. M. Cerimele, M. L. Chiofalo, F. Pistella, S. Succi, and M. P. Tosi, Phys. Rev. E **62**, 1382 (2000).
[19] M. M. Cerimele, F. Pistella, and S. Succi, Comput. Phys. Commun. **129**, 82 (2000).
[20] P. A. Ruprecht, M. J. Holland, K. Burnett, and M. Edwards, Phys. Rev. A **51**, 4704 (1995).
[21] J. R. Ensher, D. S. Jin, M. R. Matthews, C. E. Wieman, and E. A. Cornell, Phys. Rev. Lett. **77**, 4984 (1996).
[22] H. Wang, Appl. Math. Comput. **170**, 17 (2005).
[23] W. Bao, S. Jin, and P. A. Markowich, J. Comput. Phys. **175**, 487 (2002).
[24] W. Bao, S. Jin, and P. A. Markowich, SIAM J. Sci. Comput. (USA) **25**, 27 (2003).
[25] W. Bao, D. Jaksch, and P. A. Markowich, J. Comput. Phys. **187**, 318 (2003).
[26] W. Bao and J. Shen, SIAM J. Sci. Comput. (USA) **26**, 2010 (2005).
[27] A. Aftalion and Q. Du, Phys. Rev. A **64**, 063603 (2001).
[28] M. L. Chiofalo, S. Succi, and M. P. Tosi, Phys. Rev. E **62**, 7438 (2000).
[29] W. Bao and Q. Du, SIAM J. Sci. Comput. (USA) **25**, 1674 (2004).
[30] L. Landau and E. Lifshitz, *Relativistic Quantum Field Theory* (Pergamon, Oxford, 1960).
[31] A. D. Jackson, G. M. Kavoulakis, and C. J. Pethick, Phys. Rev. A **58**, 2417 (1998).
[32] P. Leboeuf and N. Pavloff, Phys. Rev. A **64**, 033602 (2001).
[33] W. Bao and W. Tang, J. Comput. Phys. **187**, 230 (2003).
[34] S. K. Adhikari, Phys. Rev. E **62**, 2937 (2000).
[35] J. W. Goodman, in *Laser Speckle and Related Phenomena* (Springer-Verlag, Berlin, 1975), Chap. 2.
[36] J. M. Huntley, Appl. Opt. **28**, 4316 (1989).
[37] P. Horak, J. Y. Courtois, and G. Grynberg, Phys. Rev. A **58**, 3953 (1998).
[38] J. Billy, V. Josse, Z. Zuo, A. Bernard, B. Hambrecht, P. Lugan, D. Clément, L. Sanchez-Palencia, P. Bouyer, and A. Aspect, Nature (London).
[39] P. Lugan, D. Clément, P. Bouyer, A. Aspect, and L. Sanchez-Palencia, Phys. Rev. Lett. **99**, 180402 (2007).